Supplementary Information for

Mechanical checkpoint regulates monocyte differentiation in fibrotic niches

Authors: <u>Kyle H. Vining[1,2,3]</u>, <u>Anna E. Marneth[4]</u>, Kwasi Adu-Berchie[1,2], Joshua M. Grolman[1,2]‡, Christina M. Tringides[5,6], Yutong Liu[1,2], Waihay J. Wong[3,7], Olga Pozdnyakova[7]‡‡, Mariano Severgnini[8], Alexander Stafford[2], Georg N. Duda[2,9,10], F. Stephen Hodi[3], Ann Mullally[4,3], Kai W. Wucherpfennig[11]*, David J. Mooney[1,2]*

<u>Underline indicates authors contributed equally</u>

*Correspondence to: kai_wucherpfennig@dfci.harvard.edu and mooneyd@seas.harvard.edu

This PDF file includes:

Supplementary Methods

Supplementary Figures 1 to 8

Supplementary Tables 1 to 9

Supplementary References

Supplemental Methods

Bulk RNA-seq analysis for human samples in Figure S4

Gene counts from bulk human RNA sequencing were Rlog transformed [1]. For differential expression analysis, classic tools such as DESeq2 could not be used because each condition had a single replicate. Instead, variance in expression levels across experimental conditions for each gene was determined. Genes with variances≥0.3 were selected as significant for further studies. Heatmap for expression levels of selected genes was then plotted using pheatmap with hierarchical clustering in R [2]. Genes of interest were then put into the ENCODE ChIP-Seq database using ChEA3 [3] to identify transcriptional regulators.

Fabrication of macroporous collagen-alginate scaffolds

Mixtures of alginate, collagen, and calcium carbonate were obtained as described in the main text methods, and then cast onto 20 mm diameter microwells of a 6-well MatTek plate. The mixture was allowed to ionically crosslink for 45 min before gels were frozen at −80 °C and lyophilized to create a porous structure, as previously described [4]. Primary bone marrow human monocytes (~1×10^6 cells) in HBSS, 20 mM HEPES, pH 7.4 were then seeded onto the porous scaffolds in 100 uL and incubated for 60 min before adding full culture media. Cells were retrieved for analysis as described in main text methods.

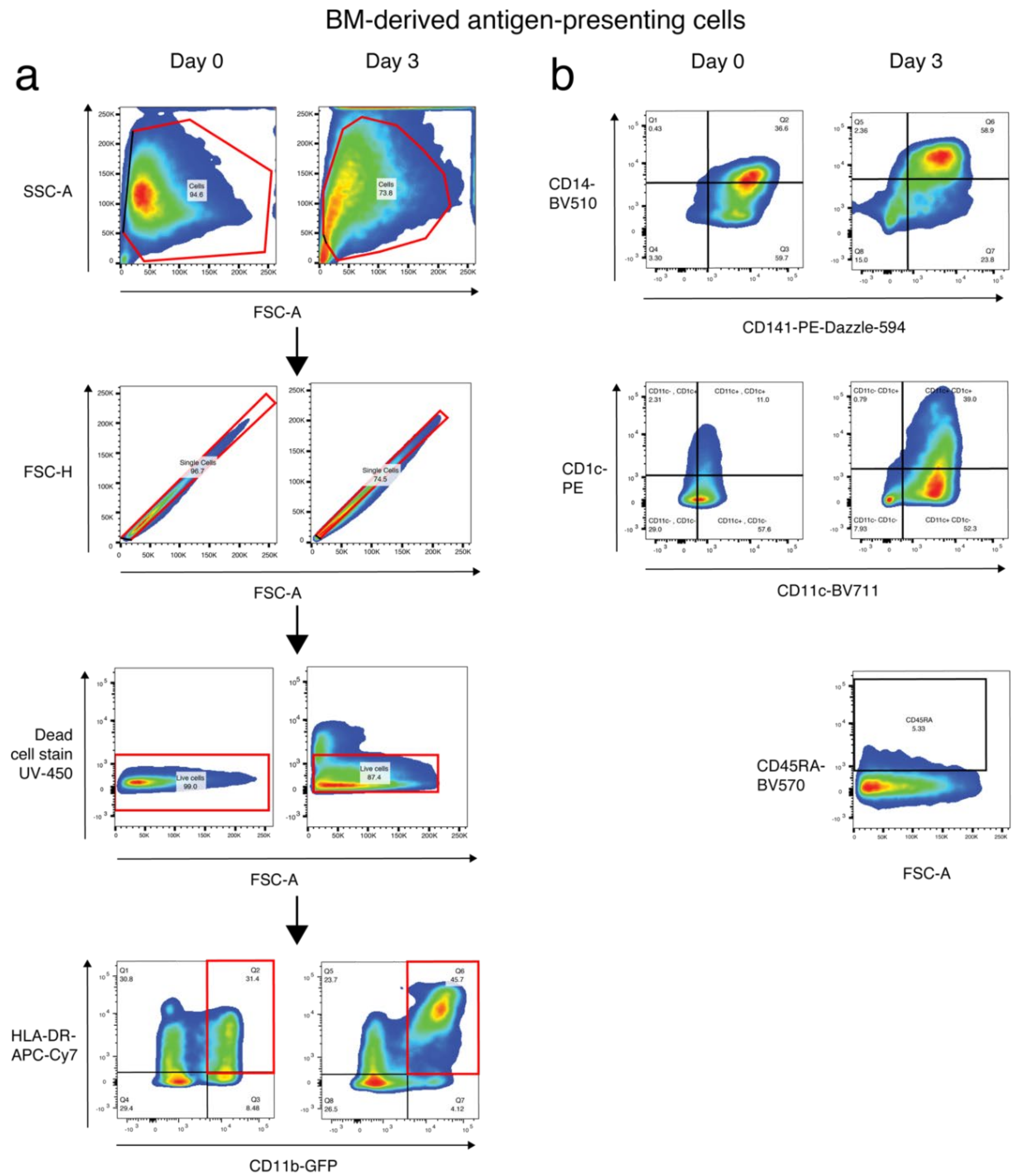

Supplementary Figure 1. Related to Figures 2 and 3. Antigen-presenting cells, positive for CD11b+ HLA-DR+ CD14+ CD141+ and negative for plasmocytoid dendritic cell marker CD45RA, were enriched from fresh human bone marrow mononuclear cells with cytokines GM-CSF, IL4 and PGE2. **A)** Gating strategy of enriched monocytes after overnight incubation at Day 0 and at Day 3 in non-adherent culture with GM-CSF, IL4, and PGE2. Applies to Fig. 2a-b, Fig. 3a-f, and h, Fig. 4f-g **B)** Plots were gated on CD11b+ HLA-DR+ cells and analyzed for CD14, CD141, CD11c, CD1c, and CD45RA at Day 0 and Day 3.

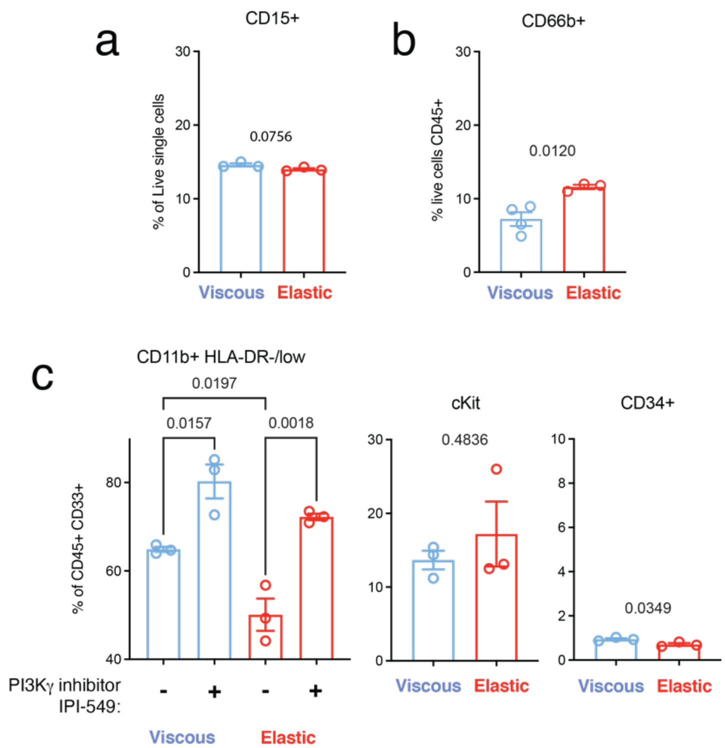

Supplementary Figure 2. Related to Figure 3. Flow cytometry of immature myeloid markers in viscous and elastic matrices. **A-B)** Fraction of cells expressing neutrophil markers CD15 **(A)** and CD66b **(B)**, gated on live and live CD45+ cells, respectively. HLA-DR and CD11b with quantification of HLA-DR mean fluorescence intensity (MFI) on the right, gated on live cells. P-values<0.05 indicate statistically significant difference by unpaired two-tailed Student's t test, n=3 biological replicates from a single donor. **C)** Fraction of cells expressing immature markers CD11b+ HLA-DR-/low, and stem/progenitor markers c-Kit and CD34, gated on live CD45+CD33+ cells. Cells were treated with 10 µM IPI-549 in the left panel of **(C)**. Data points indicate n=3 biological replicates from a single donor. P-values <0.05 indicate statistically significant differences of unpaired two-tailed Student's t test or one-way ANOVA with Tukey's multiple comparisons test. Analyses in gels were performed after 3 days. Data are presented as mean values +/- SEM.

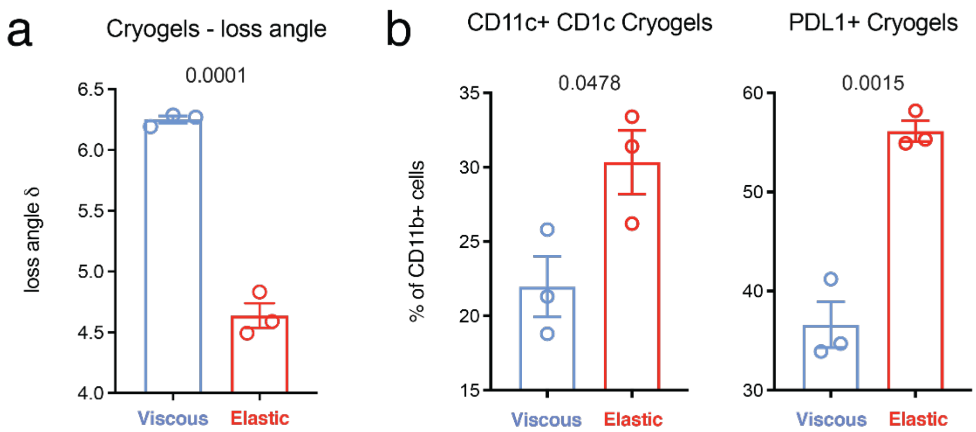

Supplementary Figure 3. Monocytes respond to viscoelasticity of macroporous elastic matrix. **A)** Loss-angle (δ) of viscous (blue) or elastic (red) macroporous hydrogels measured by oscillatory shear rheology with a 8 mm flat plate geometry under 10% pre-strain compression at 0.1% strain and 1 Hz. **B)** Fraction of CD11c+ CD1c+ conventional dendritic cells and PDL1+ cells, gated on live CD11b+ cells. P-values <0.05 indicate statistically significant differences of unpaired two-tailed Student's t test with n=3 replicates. Analyses of monocytes in gels were performed after 3 days. Data are presented as mean values +/- SEM.

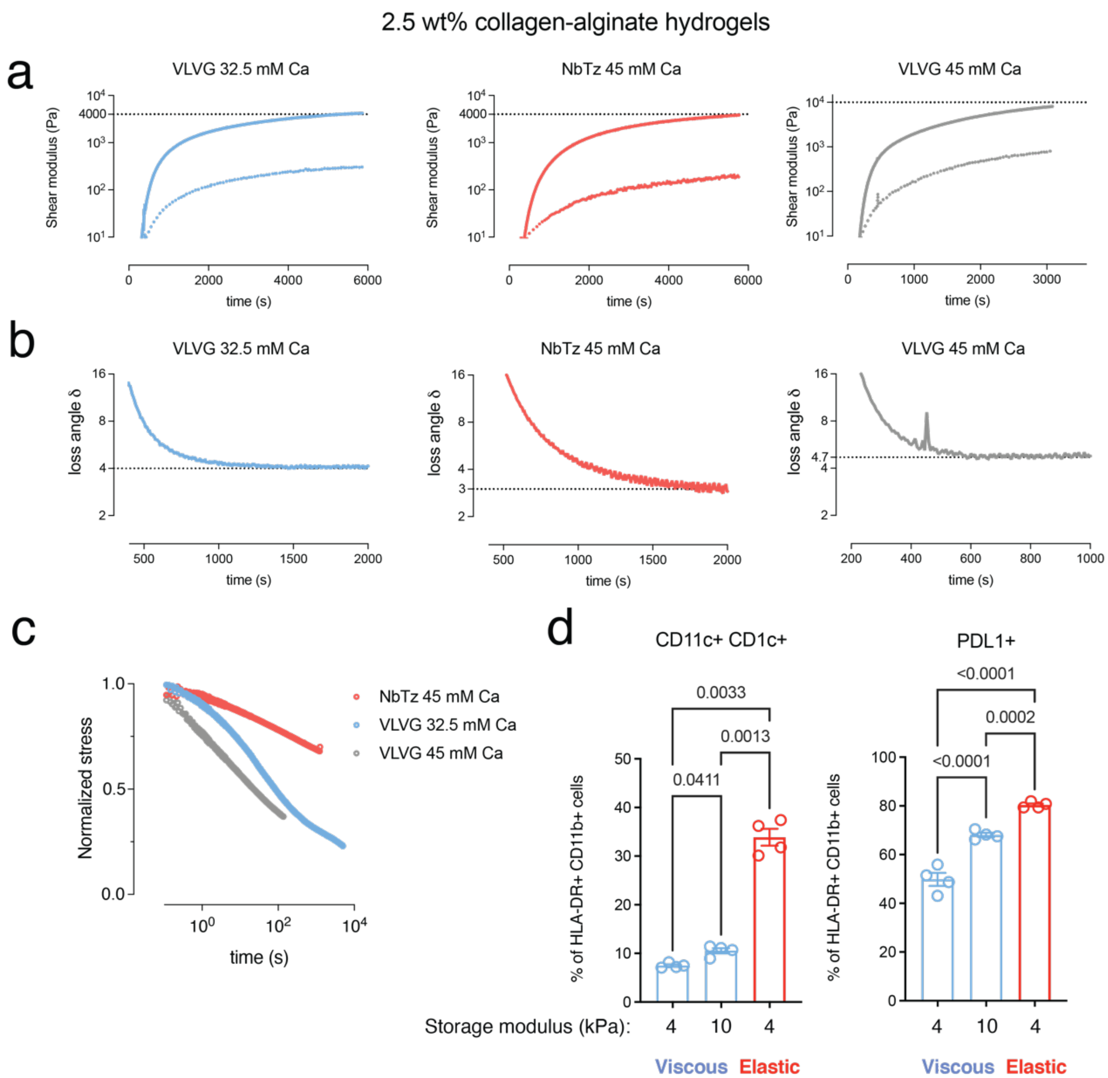

Supplementary Figure 4. Increased range of stiffness of viscous hydrogels shows similar effects on monocyte fate as softer viscous material. **A-B)** Rheology timesweeps of storage modulus **(A)** and loss-angle (δ) **(B)** of 4kPa viscous (blue) or elastic (red) and 10 kPa viscous (grey) nanoporous 2.5 wt% collagen-alginate hydrogels measured by oscillatory shear rheology at 1% strain and 1 Hz. **C)** Normalized shear stress relaxation at 15% strain of 2.5 wt% 4 kPa viscous (blue) or elastic (red) and 10 kPa viscous (grey) hydrogels. **D)** Fraction of CD11c+ CD1c+ conventional dendritic cells and PDL1+ cells, gated on live HLA-DR+ CD11b+ cells. P-values <0.05 indicate statistically significant differences of Brown-Forsythe multiple comparisons test (CD11c+ CD1c+) or one-way ANOVA with Tukey's multiple comparisons test (PDL1+) with n=4 biological replicates from 1 donor. Analyses of monocytes in gels were performed after 5 days. Data are presented as mean values +/- SEM.

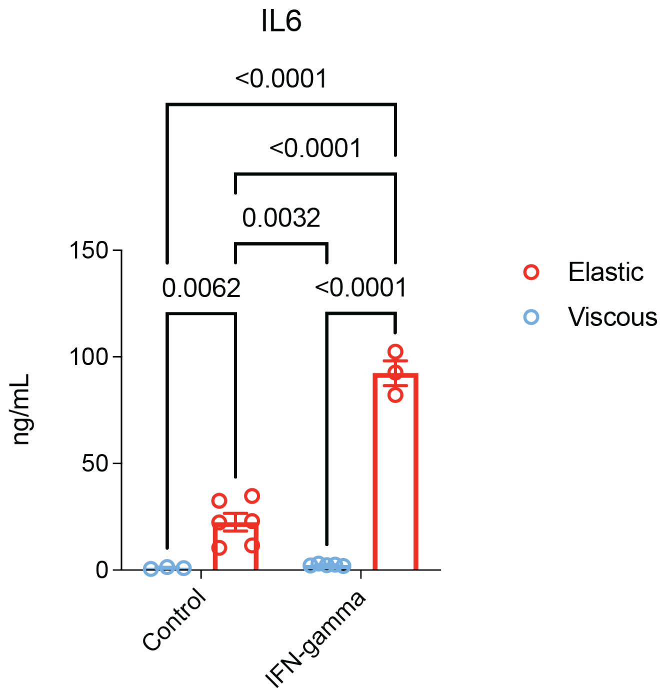

Supplementary Figure 5. IL6 is upregulated in elastic hydrogels with IFN-gamma stimulation (100 ng/mL) after 24 hours in culture. Data points indicate biological replicates from n=1 donor. P-values <0.05 indicate statistically significant differences of two-way ANOVA with Tukey's multiple comparisons test. Data are presented as mean values +/- SEM.

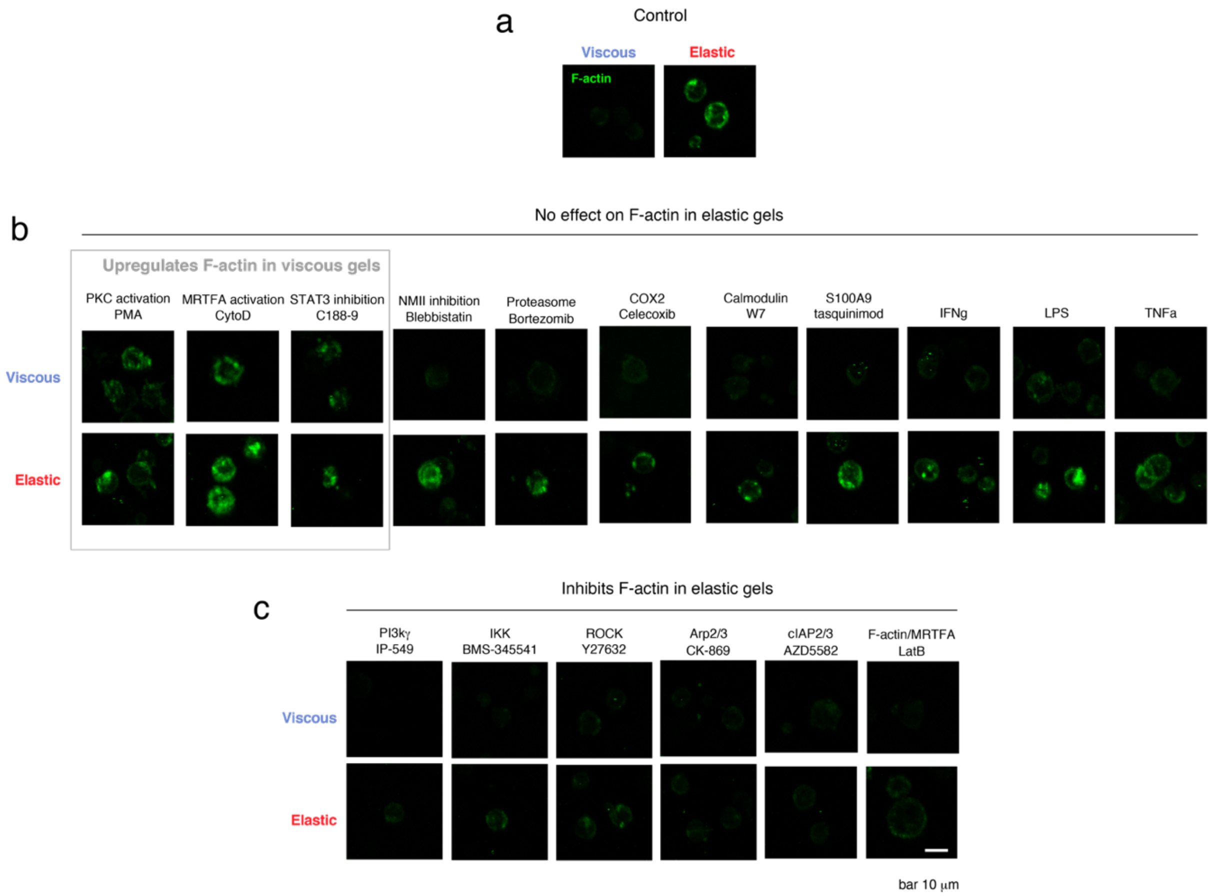

Supplementary Figure 6. Related to Figure 4. Chemical and biochemical perturbation alters F-actin cytoskeleton of monocytes in viscous and elastic hydrogels. Cells were treated with panel of cytokines and inhibitors listed in Table S3. F-actin staining (green) of monocytes in viscous and elastic hydrogels (7.5 kPa elastic modulus). Images are maximum intensity projections of representative cells. Scale bar 10 um. All analyses were performed at 3 days after encapsulation. **A)** Control cells with no cytokines or inhibitors in elastic and viscous gels. The treatment conditions are grouped by part **(B)**, demonstrating inhibitors and cytokines that either had no effect on F-actin in elastic gels, or upregulated F-actin in viscous gels (PMA, CytoD, and C188-9), and part **(C)**, demonstrating agents inhibiting F-actin assembly in elastic gels.

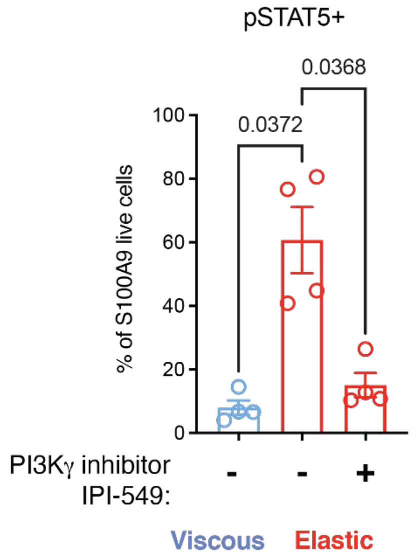

Supplementary Figure 7. Related to Figure 4. Flow cytometry of fraction of pSTAT5 positive cells in viscous or elastic gels, gated on live S100A9 cells. Cells were treated with 10 μM IPI-549 as indicated (+). Data points indicate n=4 biological replicates from 1 donor. P-values <0.05 indicate statistically significant differences of one-way Brown-Forsythe and Welch ANOVA with multiple comparisons test. Analyses in gels were performed after 3 days. Data are presented as mean values +/- SEM.

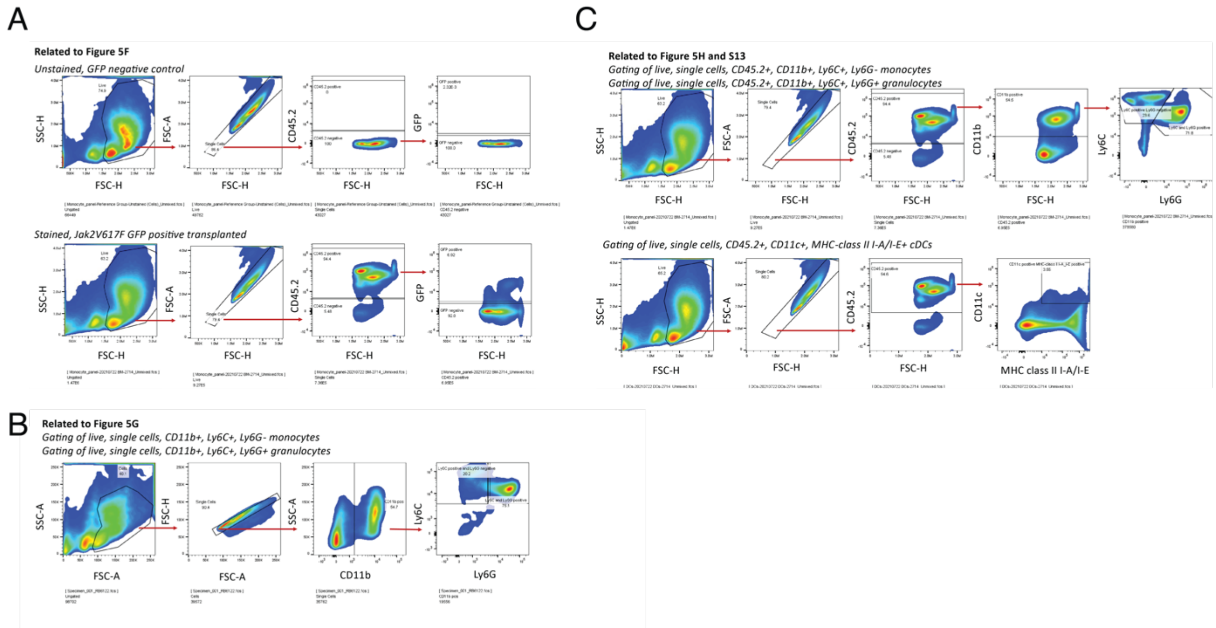

Supplementary Figure 8. Related to Figure 5. Gating strategy of flow cytometry analysis of in vivo experiments. **A)** Gating of Jak2V617F GFP+ cells in Figure 5F. **B)** Gating of Ly6C+ Ly6G- monocytes and Ly6C+Ly6G+ granulocytes in Figure 5G. **C)** Gating of CD45.2+ Ly6G- monocytes and Ly6C+Ly6G+ granulocytes (top) and cDCs (bottom) in Figure 5H and Supplementary Figure 13.

Supplementary Table 1. Formulations of artificial ECM hydrogels.

Hydrogel	Collagen (mg/mL)	Total alginate (% w/v)	VLVG alginate (% w/v)	Nb-alginate (% w/v)	Tz-alginate (% w/v)	$CaCO_3$ (% w/v)	GDL (mM)	Nb:Tz ratio	Elastic modulus* (kPa) ~~(12)~~
Soft viscous	4	1.5	1.5	0	0	0.10	40	n/a	0.75
Stiff viscous	4	1.5	1.5	0	0	0.30	120	n/a	7.5
Soft elastic	4	1.5	0.5	0.2	0.8	0.10	40	0.25	0.75
Stiff elastic	4	1.5	0	0.75	0.75	0.30	120	1.0	7.5

* Effective elastic modulus = $2G'(1 + \nu)$; G', storage modulus; $\nu=0.5$.

Supplementary Table 2. Human bone marrow donors.

Data	Donor	Lot	Age	Gender	Race
Fig. 2A	Donor 8	0000847823	30	Female	AA
Fig. 2B	Donor 2	0000760557	21	Male	AA
Fig. 2C	Donor 1	0000732183	22	Male	AA
Fig. 2D-F	Donor 1	0000732183	22	Male	AA
	Donor 2	0000760557	21	Male	AA
Fig. 3A-E	Donor 3	0000770348	24	Female	AA
Fig. 3F – CD68+ and CD11c+ CD163+	Donor 8	0000847823	30	Female	AA
Fig. 3F – SLAMF7	Donor 9	0000932523	27	Male	AA
Fig. 3G	Donor 5	0000805152	24	Male	AA
Fig. 3H	Donor 9	0000932523	27	Male	AA
Fig. 3I	Donor 2	0000760557	21	Male	AA
	Donor 3	0000770348	24	Female	AA
Fig. 4A	Donor 2	0000760557	21	Male	AA
	Donor 3	0000770348	24	Female	AA
Fig. 4B-C images	Donor 4	0000789470	22	Male	AA
Fig. 4C scatterplot	Donor 7	0000817985	27	Male	O
Fig. 4D	Donor 7	0000817985	27	Male	O
Fig. 4E	Donor 5	0000805152	24	Male	AA
Fig. 4F	Donor 5	0000805152	24	Male	AA
Fig. 4G	Donor 12	0000978383	31	Female	AA
Fig. 5B	Donor 6	0000814631	30	Male	O
	Donor 7	0000817985	27	Male	O
Extended Data Fig. 1	Donor 1	0000732183	22	Male	AA
	Donor 2	0000760557	21	Male	AA
Extended Data Fig. 2	Donor 1	0000732183	22	Male	AA
	Donor 2	0000760557	21	Male	AA
	Donor 3	0000770348	24	Female	AA
Extended Data Fig. 3A-B	Donor 10	0000643483	25	Male	H
Extended Data Fig. 3C	Donor 7	0000817985	27	Male	O

Extended Data Fig. 3D	Donor 1	0000732183	22	Male	AA
	Donor 2	0000760557	21	Male	AA
Extended Data Fig. 4A	Donor 11	0000920289	28	Male	AA
Extended Data Fig. 4B	Donor 2	0000760557	21	Male	AA
Extended Data Fig. 4C	Donor 4	0000789470	22	Male	AA
Extended Data Fig. 4D	Donor 3	0000770348	24	Female	AA
Suppl. Fig. 1	Donor 1	0000732183	22	Male	AA
Suppl. Fig. 2A	Donor 6	0000814631	30	Male	O
Suppl. Fig. 2B	Donor 14	0001038389	24	Male	AA
Suppl. Fig. 2C	Donor 13	0001011086	33	Male	C
Suppl. Fig. 3-4	Donor 14	0001020534	22	Female	O
Suppl. Fig. 5	Donor 4	0000789470	22	Male	AA
Suppl. Fig. 6	Donor 4	0000789470	22	Male	AA
Suppl. Fig. 7	Donor 14	0001020534	22	Female	O

Supplementary Table 3. Pharmacological inhibitors and cytokine treatments.

Name	Synonyms	Catalog #	Target	Concentration	Stock	Manufacturer
tasquinimod	ABR-215050	S7617	S100A9 binding to TLR4	50 uM	50 mM	Selleckchem
IKK inhibitor	BMS-345541		IKK	5 uM	50 mM	
blebbistatin			NMII	10 uM	50 mM	
ROCK inhibitor	Y-27632		ROCK	10 uM	10 mM	
Bortezomib	PS-341	S1013	Proteasome	10 nM	10 mM	Selleckchem
Cytochalasin D	CytoD	C8273	F actin depolymerization	5 uM	5 mM	
Latrunculin B	LatB	39741	F actin stabilization	1.0 uM	10 mM	Tocris
IP-549	IP549	S8330	PI3K-gamma inhibitor	1 uM	10 mM	Selleckchem
C188-9	C188-9	S8605	STAT3 inhibitor	30 uM	50 mM	Selleckchem
PMA	PMA	P1585	PKC activator; blocks F-actin	162 nM	10 mM	Sigma
LPS	LPS	L4391	TLR4 agonist	1 ug/mL	1 ug/uL	Sigma
IFN-gamma	IFN-gamma		activates TNFalpha/TGFbeta	100 ng/mL	20 ng/uL	
CK-869	CK-869	4984	Arp2/3	100 uM	100 mM	Tocris
AZD5582	AZD5582	S7362	cIAP1/2	5 uM	5 mM	Selleckchem
W7	sc-201501	sc-201501	Calmodulin	20 uM	50 mM	Scbt
Celecoxib	3786	3786	COX2	10 uM	10 mM	R&D
TNFa	TNFa		TNF receptor	100 U/mL	10 U/uL	

Supplementary Table 4. Clinical trials investigating IPI-549.

NCT number	Conditions	Interventions
NCT03795610	Head and Neck Squamous Cell Carcinoma (HPV+ and HPV-)	IPI-549
NCT03980041	Bladder Cancer Urothelial Carcinoma Solid Tumor Advanced Cancer	IPI-549, Nivolumab, Placebos
NCT02637531	Advanced Solid Tumors Non-small Cell Lung Cancer Melanoma Squamous Cell Cancer of the Head and Neck Triple Negative Breast Cancer Adrenocortical Carcinoma Mesothelioma High-circulating Myeloid-derived Suppressor Cells	IPI-549, Nivolumab
NCT03961698	Breast Cancer Renal Cell Carcinoma	IPI-549, Atezolizumab, nab-paclitaxel, Bevacizumab
NCT03719326	TNBC - Triple-Negative Breast Cancer Ovarian Cancer	AB928, IPI-549, Pegylated liposomal doxorubicin, nanoparticle albumin-bound paclitaxel

Supplementary Table 5. Significant pathways enriched by elasticity in Jak2-V617F monocytes.

Pathway	P value	Q value
mmu00100 Steroid biosynthesis	0.000126502	0.020366871
mmu04810 Regulation of actin cytoskeleton	0.000826272	0.066514923
mmu04141 Protein processing in endoplasmic reticulum	0.003405617	0.175071627
mmu04144 Endocytosis	0.004349606	0.175071627
mmu04350 TGF-beta signaling pathway	0.006905444	0.201043481
mmu00900 Terpenoid backbone biosynthesis	0.008082702	0.201043481
mmu04510 Focal adhesion	0.009049598	0.201043481
mmu04630 Jak-STAT signaling pathway	0.009989738	0.201043481
mmu04010 MAPK signaling pathway	0.011301186	0.202165669
mmu04530 Tight junction	0.014782141	0.237992472
mmu04740 Olfactory transduction	0.022715283	0.332469148
mmu04620 Toll-like receptor signaling pathway	0.027775156	0.340707778
mmu04910 Insulin signaling pathway	0.028762721	0.340707778
mmu04062 Chemokine signaling pathway	0.03117042	0.340707778
mmu04012 ErbB signaling pathway	0.032897885	0.340707778
mmu04320 Dorso-ventral axis formation	0.033859158	0.340707778
mmu04340 Hedgehog signaling pathway	0.036987263	0.350291142
mmu04662 B cell receptor signaling pathway	0.039181195	0.350454022
mmu04621 NOD-like receptor signaling pathway	0.042585999	0.351282978
mmu04360 Axon guidance	0.043637637	0.351282978
mmu04670 Leukocyte transendothelial migration	0.046269776	0.35473495
mmu04920 Adipocytokine signaling pathway	0.070865494	0.518606566
mmu04976 Bile secretion	0.074100007	0.518700052
mmu04660 T cell receptor signaling pathway	0.084909062	0.53317689
mmu04330 Notch signaling pathway	0.084928011	0.53317689
mmu04722 Neurotrophin signaling pathway	0.0861031	0.53317689
mmu04380 Osteoclast differentiation	0.091937857	0.548222037

Supplementary Table 6. Significant pathways enriched in viscous hydrogels in Jak2-V617F monocytes.

Pathway	**P value**	**Q value**
mmu03010 Ribosome	2.50E-08	4.02E-06
mmu00190 Oxidative phosphorylation	0.0031133	0.250620672
mmu00760 Nicotinate and nicotinamide metabolism	0.007212543	0.329530722
mmu04142 Lysosome	0.008187099	0.329530722
mmu00240 Pyrimidine metabolism	0.018524637	0.596493306

Supplementary Table 7. Genes enriched in elastic hydrogels in Jak2-V617F monocytes.

Gene symbol	PANTHER molecular function	Category	Log2 Fold change vs viscous gels	Adj P value
Ereg	Proepiregulin	Growth factor	3.835940598	0.015499305
Arhgef3	Rho guanine nucleotide exchange factor 3	Rho pathway	0.731307872	0.016998345
Areg	Amphiregulin	Growth factor	3.408225655	0.029073796
Acvrl1	Serine/threonine-protein kinase receptor R3	TGF-beta recetpor serine/threonine protein kinase receptor	1.058920167	0.032084746
Dpysl2	Dihydropyrimidinase-related protein 2	metalloprotease	0.702704318	0.038874481
Rhob	Rho-related GTP-binding protein RhoB	Rho pathway	1.259725058	0.069730211

Supplementary Table 8. Genes enriched in viscous hydrogels in Jak2-V617F monocytes.

Gene symbol	PANTHER molecular function	Category	Log2 Fold change vs elastic gels	Adj P value
H2-Eb1	H-2 class II histocompatibility antigen, E-B beta chain	MHC II	1.407799702	6.11E-05
Ciita	MHC class II transactivator		1.435016594	0.000383511
Lilrb4a	Leukocyte immunoglobulin-like receptor subfamily B member 4		1.098861559	0.00394989
H2-Aa	H-2 class II histocompatibility antigen, A-K alpha chain	MHC II	1.272826974	0.025815262
Mx1	Interferon-induced GTP-binding protein Mx1	Interferon signaling	0.862592772	0.029073796
Ccnd1	G1/S-specific cyclin-D1	Cell cycle	2.15214005	0.055162012

Supplementary Table 9. Statistical tests in data of main figures.

Data	Test	Passed Normality test?	Variances significantly different (p < 0.05)?	Data analyzed	P-value*
Fig. 1F	Unpaired t test, Welch correction, two-tailed	Yes	Yes	Alg – 5, NbTz - 6	**0.0227**
Fig. 1G - modulus	Unpaired t test, two-tailed	Yes	No	Alg – 5, NbTz - 12	0.3720
Fig. 1G – loss angle	Unpaired t test, two-tailed	Yes	No	Alg – 5, NbTz - 12	**0.0012**
Fig. 2A	Unpaired t test, two-tailed	Yes	No	3 each	**<0.0001**
Fig. 3C-F	Unpaired t test, two-tailed	Yes	No	3 each	**See chart**
Fig. 3G	Mann Whitney non-parametric test, two-tailed	No	n/a	Viscous – 89, Elastic - 95	**<0.0001**
Fig. 3H	Ordinary one-way ANOVA Tukey's multiple comparisons	Yes	No	3 each	
				Viscous control vs Viscous C188-9	0.9569
				Viscous control vs Elastic control	**<0.0001**
				Viscous control vs Elastic C188-9	**<0.0001**
				Viscous IPI-549 vs Elastic control	**<0.0001**
				Viscous IPI-549 vs Elastic C188-9	**<0.0001**
				Elastic control vs Elastic C188-9	**<0.0001**
Fig. 3I	Mann Whitney non-parametric test, two-tailed	No	n/a	Viscous – 57, Elastic - 22	**0.0005**
Fig. 4A	Mann Whitney non-parametric test, two-tailed	No	n/a	Viscous – 57, Elastic - 43	**<0.0001**
Fig. 4C	Mann Whitney non-parametric test, two-tailed	No	n/a	Viscous – 30, Elastic – 32	**0.0021**

Fig. 4D	Unpaired t test, Welch correction, two-tailed	Yes	Yes	Viscous – 30, Elastic – 32	**<0.0001**
Fig. 4E – % live cells	Ordinary one-way ANOVA	Yes	No	6 each	0.9838
Fig. 4E – relative cell count	Ordinary one-way ANOVA	Yes	No	6 each	0.8823
Fig. 4F – gMFI of HLA-DR-APC-Cy7	Ordinary one-way ANOVA	Yes	No	3 each	
	Tukey's multiple comparisons			Viscous control vs Viscous IPI-549	0.0553
				Viscous control vs Viscous ROCK	0.9640
				Viscous IPI-549 vs Viscous ROCK	0.1960
				Viscous control vs Elastic control	**<0.0001**
				Viscous control vs Elastic IPI-549	0.1521
				Viscous control vs Elastic ROCK	**<0.0001**
				Viscous IPI-549 vs Elastic control	**<0.0001**
				Viscous IPI-549 vs Elastic IPI-549	**0.0007**
				Viscous ROCK vs Elastic ROCK	**<0.0001**
				Elastic ROCK vs Elastic IPI-549	**0.0053**
				Elastic control vs Elastic IPI-549	**<0.0001**
Fig. 4F – % CD11c+	Ordinary one-way ANOVA	Yes	No	3 each	
	Tukey's multiple comparisons			Viscous control vs Viscous IPI-549	**<0.0001**
				Viscous control vs Viscous ROCK	0.7122
				Viscous control vs Elastic control	**<0.0001**
				Viscous control vs Elastic IPI-549	**0.0209**
				Viscous control vs Elastic ROCK	**<0.0001**
				Viscous IPI-549 vs Viscous ROCK	**<0.0001**
				Viscous IPI-549 vs Elastic control	**<0.0001**

				Viscous IPI-549 vs Elastic ROCK	**<0.0001**
				Viscous IPI-549 vs Elastic IPI-549	**<0.0001**
				Elastic control vs Elastic ROCK	**0.0063**
				Elastic control vs Elastic IPI-549	**<0.0001**
				Elastic ROCK vs Elastic IPI-549	**0.0018**
Fig. 4G – % CD11c+CD1c+	Ordinary one-way ANOVA	Yes	No	4 each	
	Tukey's multiple comparisons			Elastic control vs Elastic IPI-549	**<0.0001**
				Elastic control vs Elastic RN-1734	**<0.0001**
				Elastic control vs Elastic TGFB1	0.9497
				Elastic IPI-549 vs Elastic RN-1734	**0.0117**
				Elastic IPI-549 vs Elastic TGFB1	**<0.0001**
				Elastic RN-1734 vs Elastic TGFB1	**<0.0001**
Fig. 5B – hIL6	Brown-Forsythe and Welch ANOVA test	Yes	Yes	3 each	
	Dunnett's T3 multiple comparisons test			Viscous control vs Viscous IPI-549	0.5584
				Viscous control vs Elastic control	**<0.0001**
				Viscous control vs Elastic IPI-549	0.0860
				Viscous IPI-549 vs Elastic control	**0.0004**
				Viscous IPI-549 vs Elastic IPI-549	0.0778
				Elastic control vs Elastic IPI-549	**0.0173**
Fig. 5B – hCCL2	Brown-Forsythe and Welch ANOVA test	Yes	Yes	3 each	
	Dunnett's T3 multiple comparisons test			Viscous control vs Viscous IPI-549	n/a
				Viscous control vs Elastic control	**0.0010**

				Viscous control vs Elastic IPI-549	**0.0343**
				Viscous IPI-549 vs Elastic control	n/a
				Viscous IPI-549 vs Elastic IPI-549	n/a
				Elastic control vs Elastic IPI-549	**0.0045**
Fig. 5B – hCCL4	Ordinary One-way ANOVA Tukey’s multiple comparisons test	Yes	No	6 for elastic gels (below limit of detection for some viscous gels, n = 2)	
				Viscous control vs Viscous IPI-549	n/a
				Viscous control vs Elastic control	n/a
				Viscous control vs Elastic IPI-549	n/a
				Viscous IPI-549 vs Elastic control	n/a
				Viscous IPI-549 vs Elastic IPI-549	n/a
				Elastic control vs Elastic IPI-549	**<0.0001**
Fig. 5B – hIL8	Brown-Forsythe and Welch ANOVA test Dunnett’s T3 multiple comparisons test	Yes	Yes	3 each	
				Viscous control vs Viscous IPI-549	0.1382
				Viscous control vs Elastic control	**<0.0001**
				Viscous control vs Elastic IPI-549	**<0.0001**
				Viscous IPI-549 vs Elastic control	**<0.0001**
				Viscous IPI-549 vs Elastic IPI-549	**<0.0001**
				Elastic control vs Elastic IPI-549	**<0.0001**
Fig. 5D - WBC	Unpaired t test, Welch correction, two-tailed	Yes	Yes	EV – 9, Jak2-V617F – 10	**0.0253**
Fig. 5D - RBC	Unpaired t test, Welch correction, two-tailed	Yes	Yes	EV – 9, Jak2-V617F – 10	**<0.0001**
Fig. 5D - HCT	Unpaired t test, two-tailed	Yes	No	EV – 9, Jak2-V617F – 10	**0.0079**

Fig. 5D - Spleen	Unpaired t test, Welch correction, two-tailed	Yes	Yes	EV – 9, Jak2-V617F – 9	**0.0024**
Fig. 5D - Neutrophils	Unpaired t test, Welch correction, two-tailed	Yes	Yes	EV – 9, Jak2-V617F – 9	**0.0024**
Fig. 5E – G’	Brown-Forsythe and Welch ANOVA Dunnett’s T3 multiple comparisons	Yes	Yes	WT – 9, BM – 8, Jak2-V617F – 9	
				WT vs BM	0.1945
				WT vs Jak2	**0.0003**
				BM vs Jak2	**0.0011**
Fig. 5E – tan(delta)	Ordinary one-way ANOVA Tukey’s multiple comparisons	Yes	No	WT – 9, BM – 8, Jak2-V617F – 9	
				WT vs BM	0.8069
				WT vs Jak2	0.1193
				BM vs Jak2	0.3690
Fig. 5F – CD11b+	Ordinary one-way ANOVA Tukey’s multiple comparisons	Yes	No	Control– 7, Non-fibrotic Jak2-V617F – 7, Fibrotic Jak2-V617F – 5	
				Control vs Non-fibrotic	0.9784
				Control vs Fibrotic	0.9680
				Non-fibrotic vs Fibrotic	0.9122
Fig. 5F – Ly6C+Ly6G-	Ordinary one-way ANOVA Tukey’s multiple comparisons	Yes	No	Control– 7, Non-fibrotic Jak2-V617F – 7, Fibrotic Jak2-V617F – 5	
				Control vs Non-fibrotic	0.9997
				Control vs Fibrotic	**0.0010**
				Non-fibrotic vs Fibrotic	**0.0020**
Fig. 5G – Ly6C+Ly6G-	Unpaired t test, two-tailed	Yes	No	Vehicle – 4, IPI-549 – 6	**0.0484**
Fig. 5G – cDCs	Unpaired t test, two-tailed	Yes	No	Vehicle – 4, IPI-549 – 6	**0.0301**

Fig. 6	See Methods on scRNA-seq analysis for statistical test information	

***Bold P-value indicates statistically significant difference, $p<0.05$.

Supplemental References

1 Love, M. I., Huber, W. & Anders, S. Moderated estimation of fold change and dispersion for RNA-seq data with DESeq2. *Genome Biology* **15**, 550, doi:10.1186/s13059-014-0550-8 (2014).

2 pheatmap: Pretty Heatmaps v. R package version 1.0.12 (2019).

3 Keenan, A. B. *et al.* ChEA3: transcription factor enrichment analysis by orthogonal omics integration. *Nucleic Acids Research* **47**, W212-W224, doi:10.1093/nar/gkz446 (2019).

4 Qazi, T. H., Mooney, D. J., Duda, G. N. & Geissler, S. Biomaterials that promote cell-cell interactions enhance the paracrine function of MSCs. *Biomaterials* **140**, 103-114, doi:https://doi.org/10.1016/j.biomaterials.2017.06.019 (2017).